# The Poincaré-Steklov Operator in Hybrid Finite Element-Boundary Integral Equation Formulations

Pieterjan Demarcke and Hendrik Rogier, *Senior Member, IEEE.*

***Abstract*—The Poincaré-Steklov operator provides a direct relation between the tangential electric and magnetic field at the boundary of a simply connected domain, and a discrete equivalent of the operator can be constructed from the sparse finite element (FE) matrix of that domain by forming the Schur complement to eliminate the interior unknowns. Identifying the FE system matrix as a discretized version of the Poincaré-Steklov operator allows us to describe and analyze FE and hybrid finite element-boundary integral equation (FE-BIE) formulations from an operator point of view. We show how this operator notation provides substantial theoretical insight into the analysis of spurious solutions in hybrid FE-BIE methods, and we apply the theory on a TM scattering example to predict the breakdown frequencies of different hybrid formulations.**

***Index Terms*—Hybrid methods, Electromagnetic scattering**

## I. Introduction

The hybrid FE-BIE method is a widely used approach to numerically solve electromagnetic scattering or radiation problems. It combines the versatility of the FE method to model complex inhomogeneous and anisotropic structures with the accuracy and efficiency of the BIE method to model large homogeneous and potentially unbounded domains. Traditionally, the FE formulation is set in a variational framework, which is extended with the BIE formalism to form a hybrid variational formulation. However, this approach relies on the internal field densities in the FE domain, and since the exact method used to couple both formulations seems to be very important to avoid spurious solutions, we expect that a hybrid formalism specifically focusing on the behavior of the formulations at the boundary will provide more theoretical insights.

In this paper, we use the concept of a Poincaré-Steklov (PS) operator to describe the FE formulation in a domain by the relation it provides between the tangential electric and magnetic fields at the boundary of the domain. Hybrid formulations are easily formed by properly combining the PS and BIE operators. Unlike the classical variational framework, this operator notation retains the individual identities of the FE and BIE operators in FE-BIE formulations, and different properties regarding spurious solutions are easily derived. After outlining the general equations in Section II, we use the new operator notation in Section III to analyze the problem of spurious solutions in commonly used hybrid FE-BIE formulations. The theoretical results are then applied in Section IV to compare the analytical and the simulated breakdown frequencies of the different FE-BIE formulations for a TM scattering problem involving a single dielectric cylinder.

P. Demarcke and H. Rogier are with the Department of Information Technology, Ghent University, Sint-Pietersnieuwstraat 41, 9000 B-Gent, Belgium. E-mail: pieterjan.demarcke@intec.UGent.be.

## II. General Formulation

Consider the homogeneous and isotropic background medium $\Omega_0$ characterized by the electric permittivity $\epsilon_0$ and magnetic permeability $\mu_0$. Embedded in $\Omega_0$ is a cylindrical scatterer, aligned and invariant along the $z$-axis, and with arbitrary cross-section $S$ in the $xy$-plane. The inhomogeneous scatterer is characterized by the relative permittivity and permeability tensors $\bar{\bar{\epsilon}}_r(\boldsymbol{\rho})$ and $\bar{\bar{\mu}}_r(\boldsymbol{\rho})$ in each point $\boldsymbol{\rho} \in S$. At the object boundary $\partial S$, we define $C^+$ as the closed contour in $\Omega_0$ just large enough to enclose $\partial S$, and $C^-$ as the contour just small enough to be enclosed by $\partial S$. Local orthonormal coordinate systems $\left(\hat{\mathbf{n}}^+, \hat{\mathbf{t}}^+, \hat{\mathbf{z}}\right)$ and $\left(\hat{\mathbf{n}}^-, \hat{\mathbf{t}}^-, \hat{\mathbf{z}}\right)$ are defined on $C^+$ and $C^-$, respectively, with the unit normal $\hat{\mathbf{n}}^+$ pointing into $S$ and $\hat{\mathbf{n}}^-$ pointing into $\Omega_0$. All fields and sources are time-harmonic with a time dependency $e^{j\omega t}$, and to describe the governing equations, we focus on pure transverse magnetic (TM) fields $(\mathrm{e}_z\hat{\mathbf{z}}, \mathbf{h}_t)$. To simplify some expressions, we normalize the magnetic field $\mathbf{h}_t$ by the characteristic impedance $Z_0 = \sqrt{\mu_0/\epsilon_0}$ of the background medium.

### A. Boundary Integral Equation Formulation

In the homogeneous background medium, the fields at an observation point $\boldsymbol{\rho} \in \Omega_0$ are related to the tangential electric and magnetic fields at the boundary $C^+$ by means of an integral equation containing the Green's function $G_0(\boldsymbol{\rho}, \boldsymbol{\rho}')$ as integration kernel. Depending on the observed field, we differentiate between the electric and the magnetic field integral equation (EFIE and MFIE). After moving the observation point $\boldsymbol{\rho}$ towards the boundary $C^+$ and taking the limit, we obtain the well-known boundary integral equations

$$\mathrm{e}_z^{\mathrm{in}} = \frac{\mathrm{e}_z^+}{2} - \mathrm{pv}\oint_{C^+} \mathrm{e}_z^+ \frac{\partial G_0}{\partial \hat{\mathbf{n}}^{+\prime}}\,\mathrm{d}c' + jk_0 \oint_{C^+} \mathrm{h}_t^+ G_0\,\mathrm{d}c' \tag{1}$$

$$\mathrm{h}_t^{\mathrm{in}} = \frac{\mathrm{h}_t^+}{2} - \oint_{C^+} \frac{\mathrm{e}_z^+}{jk_0} \frac{\partial^2 G_0}{\partial \hat{\mathbf{n}}^+ \partial \hat{\mathbf{n}}^{+\prime}}\,\mathrm{d}c' + \mathrm{pv}\oint_{C^+} \mathrm{h}_t^+ \frac{\partial G_0}{\partial \hat{\mathbf{n}}^+}\,\mathrm{d}c', \tag{2}$$

with $\mathrm{e}_z^+ \in H^{\frac{1}{2}}(C^+)$ and $\mathrm{h}_t^+ = \mathbf{h}_t \cdot \hat{\mathbf{t}}^+ \in H^{-\frac{1}{2}}(C^+)$ the tangential electric and magnetic field on $C^+$, and $k_0$ the wave number of an incoming plane wave in $\Omega_0$ with tangential fields $\mathrm{e}_z^{\mathrm{in}}$ and $\mathrm{h}_t^{\mathrm{in}}$ on $C^+$. The Green's function is given by

$$G_0(\boldsymbol{\rho}, \boldsymbol{\rho}') = \frac{j}{4} H_0^{(2)}(k_0 \left|\boldsymbol{\rho} - \boldsymbol{\rho}'\right|), \tag{3}$$

with $H_0^{(2)}$ the 0-th order Hankel function of the second kind. Following the operator notations of [1], we write the EFIE (1) and the MFIE (2) compactly as

$$\mathcal{P}\begin{pmatrix} \mathrm{e}_z^+ \\ \mathrm{h}_t^+ \end{pmatrix} \equiv \begin{pmatrix} -\mathcal{K}_0 + \frac{1}{2} & \mathcal{G}_0 \\ -\mathcal{J}_0 & \mathcal{K}_0' + \frac{1}{2} \end{pmatrix} \begin{pmatrix} \mathrm{e}_z^+ \\ \mathrm{h}_t^+ \end{pmatrix} = \begin{pmatrix} \mathrm{e}_z^{\mathrm{in}} \\ \mathrm{h}_t^{\mathrm{in}} \end{pmatrix}. \tag{4}$$

We remark that the Calderón operator $\mathcal{P}$ in (4) is an oblique projector with eigenvalues $\{0, 1\}$ [1]. At the boundary $C^+$, the tangential electric and magnetic fields $(\mathrm{e}_z^+, \mathrm{h}_t^+)$ satisfy

$$\frac{1}{jk_0}\frac{\partial \mathrm{e}_z^+}{\partial \hat{\mathbf{n}}^+} = \mathcal{Y}_0 \mathrm{e}_z^+ = \mathrm{h}_t^+, \tag{5}$$

which is a direct consequence of Maxwell's curl equation for the electric field. In (5) we introduced the PS operator $\mathcal{Y}_0 : H^{\frac{1}{2}}(C^+) \to H^{-\frac{1}{2}}(C^+)$, also known as the Dirichlet-to-Neumann (DtN) operator. Details on this self-adjoint operator can be found in [1]. Here, we just repeat that $\mathcal{Y}_0$ satisfies, among others, $\mathcal{Y}_0 = \mathcal{G}_0^{-1}\left(\mathcal{K}_0 - \frac{1}{2}\right)$ and $\mathcal{J}_0 = \mathcal{Y}_0\left(\mathcal{K}_0 + \frac{1}{2}\right)$.

Next to $\mathcal{P}$, we also define the complementary Calderón projector $\widetilde{\mathcal{P}}$, which represents the BIE formulation in the complement of the domain of $\mathcal{P}$ (i.e. $\Omega_0 \to S$, $C^+ \to C^-$, $\mathbf{n}^+ \to \mathbf{n}^-$), with the complement filled with the same homogeneous material. From (1) and (2), it follows that this operator $\widetilde{\mathcal{P}}$ is closely related to the operator $1-\mathcal{P}$, which represents the same complementary Calderón projector, but now for fields on $C^+$. Comparing both and using the tangential field continuity $(\mathrm{e}_z^+, \mathrm{h}_t^+) = (\mathrm{e}_z^-, -\mathrm{h}_t^-)$ reveals the identity $\mathcal{Y}_0 + \mathcal{G}_0^{-1} = -\widetilde{\mathcal{Y}}_0$, which in turn leads to the identity $\widetilde{\mathcal{Y}}_0 = -\mathcal{G}_0^{-1}\left(\mathcal{K}_0 + \frac{1}{2}\right)$.

### B. Finite Element Formulation

The FE formulation consists of a weak boundary value problem (BVP) for the electric or magnetic field in $S$, with boundary conditions given by the equivalent sources on $C^-$. The solution and test function space is the finite subspace $\mathcal{W}_h \subset H(\mathrm{curl}; S)$, which is equal to the span of the set of curl-conforming basis functions $\mathbf{w}$ defined on a geometrical partitioning (mesh) of $S$ with characteristic element size $h$. With $\mathbf{u}, \mathbf{v} \in \mathcal{W}_h$, we define the scalar product over $S$ and $C^-$ as $\langle \mathbf{u}, \mathbf{v}\rangle_S = \int_S \mathbf{u}\cdot\mathbf{v}\,\mathrm{d}S$ and $\langle \mathbf{u}, \mathbf{v}\rangle_{C^-} = \oint_{C^-} \mathbf{u}\cdot\mathbf{v}\,\mathrm{d}C$, respectively. The weak form of the BVP for the electric and magnetic field is given by

$$\begin{aligned}\left\langle \nabla_t \times \mathrm{w}_n\hat{\mathbf{z}}\,,\, \overline{\overline{\mu}}_r^{-1}\cdot\nabla_t\times \mathrm{e}_z\hat{\mathbf{z}}\right\rangle_S - k_0^2\left\langle \mathrm{w}_n\hat{\mathbf{z}}\,,\, \epsilon_{r,zz}\mathrm{e}_z\hat{\mathbf{z}}\right\rangle_S \\ = jk_0\left\langle \mathrm{w}_n\hat{\mathbf{z}}\,,\, \hat{\mathbf{n}}^-\times\mathbf{h}_t\right\rangle_{C^-}\end{aligned} \tag{6}$$

$$\begin{aligned}\left\langle \nabla_t\times\mathbf{w}_e\,,\, \epsilon_{r,zz}^{-1}\nabla_t\times\mathbf{h}_t\right\rangle_S - k_0^2\left\langle \mathbf{w}_e\,,\, \overline{\overline{\mu}}_r\cdot\mathbf{h}_t\right\rangle_S \\ = jk_0\left\langle \mathbf{w}_e\,,\, \mathrm{e}_z\hat{\mathbf{z}}\times\hat{\mathbf{n}}^-\right\rangle_{C^-},\end{aligned} \tag{7}$$

where we assumed $S$ to be source-free. The scalar node basis functions $\mathrm{w}_n$ in the electric field formulation (EFF) (6) and the vector-valued edge basis functions $\mathbf{w}_e$ in the magnetic field formulation (MFF) (7) ensure tangential field continuity along mesh element boundaries for the $\mathrm{e}_z$ and $\mathbf{h}_t$ fields, respectively.

To model the influence of $S$ on the scattered and radiated fields in and around $S$, we can express the relation between the tangential electric and magnetic field at $C^-$ in terms of a PS operator $\mathcal{Y}_1$ associated with $S$. Similarly as in (5), we have $\mathcal{Y}_1\mathrm{e}_z^- = \mathrm{h}_t^-$, and for $\overline{\overline{\mu}}_r$ isotropic at $C^-$, we find again the DtN operator. Although the EFF (6) and its sparse FE system explicitly depend on the inner electric field distribution, an equivalent direct relation between $\mathrm{e}_z^-$ and $\mathrm{h}_t^-$ is found after forming the Schur complement to eliminate the interior degrees of freedom in the sparse FE matrix. Formally, this elimination does not change the total field solution, hence the sparse and the compressed FE matrices associated with (6) can be interpreted as being different discretizations of the same PS operator $\mathcal{Y}_1$. It follows that we can represent the EFF and MFF analytically by the operator equations

$$\mathcal{F}\begin{pmatrix}\mathrm{e}_z^-\\ \mathrm{h}_t^-\end{pmatrix} \equiv \begin{pmatrix}0 & \mathcal{Y}_1^{-1}\\ \mathcal{Y}_1 & 0\end{pmatrix}\begin{pmatrix}\mathrm{e}_z^-\\ \mathrm{h}_t^-\end{pmatrix} = \begin{pmatrix}\mathrm{e}_z^-\\ \mathrm{h}_t^-\end{pmatrix}. \tag{8}$$

Remark that the Hamiltonian operator $\mathcal{F}$ satisfies $\mathcal{F}^2 = 1$, with eigenvalues $\{-1, 1\}$. Unlike the variational approach, the new operator notation for the FE formulation does not depend on any definition of mesh or basis function, which allows us to make abstraction of all discretization issues while analyzing the FE and hybrid FE-BIE formulations.

Finally, we remark that at frequencies where one of the PS operators (i.e. $\mathcal{Y}_1$) becomes singular, its inverse $\mathcal{Y}_1^{-1}$ is not uniquely defined, which is reflected in a singular submatrix for the interior-to-interior interactions that makes the Schur complement undefined. Hence, to obtain a valid representation for $\mathcal{Y}_1^{-1}$ at the operator level when $\mathcal{Y}_1$ is singular, we implicitly assume the extension of $C^-$ with some line segment at the interior of $S$, which is the equivalent of leaving some unknowns uneliminated while forming the Schur complement.

## III. Analysis of Hybrid FE-BIE Formulations

Considering that (4) and (8) each consist of two independent equations, different options are available to combine (some of) these into a hybrid FE-BIE formulation. While the individual EFIE or MFIE is almost always sufficient to properly enforce the BIE formulation at $C^+$, at specific frequencies both are needed to guarantee uniqueness. Consequently, we will always use both the EFIE and the MFIE in the FE-BIE formulations.

Expressing the tangential field continuity between $C^-$ and $C^+$ simply as $\mathrm{e}_z^- = \mathrm{e}_z^+$ and $\mathrm{h}_t^- = -\mathrm{h}_t^+$, we can substitute the EFIE into the right hand side of (7) and combine the result with the MFIE. By splitting $\mathrm{e}_z^-$ in the right-hand side of (7) in two before substitution, a symmetric hybrid FE-BIE formulation is found. In our operator notation, we obtain

$$\begin{pmatrix}-\mathcal{J}_0 & \mathcal{K}_0' + \frac{1}{2}\\ \mathcal{K}_0 + \frac{1}{2} & -\mathcal{G}_0 + \mathcal{Y}_1^{-1}\end{pmatrix}\begin{pmatrix}\mathrm{e}_z^+\\ \mathrm{h}_t^+\end{pmatrix} = \begin{pmatrix}\mathrm{h}_t^{\mathrm{in}}\\ -\mathrm{e}_z^{\mathrm{in}}\end{pmatrix}. \tag{9}$$

While the variational or discrete equivalent of (9) was repeatedly mentioned in literature, it suffers from spurious solutions in the $\mathrm{e}_z^+$ field component at certain resonant frequencies, while the $\mathrm{h}_t^+$ component remains unaffected. This was also observed in [2], and a sound theoretical explanation follows after careful analysis of the operators in (9). From $\mathcal{J}_0 = \mathcal{Y}_0\left(\mathcal{K}_0 + \frac{1}{2}\right)$, it follows that the elements of the null space of $\mathcal{K}_0 + \frac{1}{2}$ (denoted $\mathcal{N}\left(\mathcal{K}_0 + \frac{1}{2}\right)$) are eigenvectors of $\mathcal{J}_0$ with 0 as eigenvalue. Consequently, at specific resonant frequencies, the solution of (9) will only be defined up to a spurious tangential electric field proportional to $\mathrm{e}_z^{\mathrm{sp}} \in \mathcal{N}\left(\mathcal{K}_0 + \frac{1}{2}\right)$. Since $\widetilde{\mathcal{Y}}_0\mathrm{e}_z^{\mathrm{sp}} = -\mathcal{G}_0^{-1}\left(\mathcal{K}_0 + \frac{1}{2}\right)\mathrm{e}_z^{\mathrm{sp}} = 0$, we find that these resonant frequencies are eigenfrequencies of the Neumann eigenmodes of $S$ filled with background material.

A formulation dual to (9) can be found by substituting the MFIE into (6) and combining the result with the EFIE. This formulation has equivalent problems as (9), but now at Dirichlet eigenfrequencies with $\mathcal{G}_0$ and $\mathcal{K}_0' - \frac{1}{2}$ singular, giving rise to a spurious tangential magnetic field. Between both, (9) is preferred since the dispersion error due to the finite mesh in $S$ is smaller for edge element basis functions [3].

It seems that spurious solutions in (9) exist because the MFIE is not coupled with a FE counterpart. Similarly as for the BIE formulation, one would expect that uniqueness follows after using both the EFF and the MFF in $S$. We obtain

$$\begin{pmatrix} -\mathcal{J}_0 - \frac{1}{2}\mathcal{Y}_1 & \mathcal{K}_0' \\ \mathcal{K}_0 & -\mathcal{G}_0 + \frac{1}{2}\mathcal{Y}_1^{-1} \end{pmatrix} \begin{pmatrix} \mathrm{e}_z^+ \\ \mathrm{h}_t^+ \end{pmatrix} = \begin{pmatrix} \mathrm{h}_t^{\mathrm{in}} \\ -\mathrm{e}_z^{\mathrm{in}} \end{pmatrix}. \tag{10}$$

While simulations with (10) confirm that no spurious solutions are present at the Dirichlet and Neumann eigenfrequencies, resonances do exist elsewhere. This unexpected result can again be explained by careful analysis of the FE and BIE operators and their interactions. After rewriting (10) as

$$\left(\mathcal{P} - \frac{1}{2}(1 + \mathcal{F})\right) \begin{pmatrix} \mathrm{e}_z^+ \\ \mathrm{h}_t^+ \end{pmatrix} = \begin{pmatrix} \mathrm{e}_z^{\mathrm{in}} \\ \mathrm{h}_t^{\mathrm{in}} \end{pmatrix},$$

the spurious solutions seem to be the elements of the null-space $\mathcal{N}\big(\mathcal{P} - \frac{1}{2}(1 + \mathcal{F})\big)$. Since $\mathcal{P}$ and $\frac{1}{2}(1 + \mathcal{F})$ both have eigenvalues $\{0, 1\}$, spurious solutions to (10) will exist if we can find a couple $(\mathrm{e}_z^{\mathrm{sp}}, \mathrm{h}_t^{\mathrm{sp}})$ that satisfy either

$$\mathcal{P} \begin{pmatrix} \mathrm{e}_z^{\mathrm{sp}} \\ \mathrm{h}_t^{\mathrm{sp}} \end{pmatrix} = 0 = (1 + \mathcal{F}) \begin{pmatrix} \mathrm{e}_z^{\mathrm{sp}} \\ \mathrm{h}_t^{\mathrm{sp}} \end{pmatrix}, \tag{11}$$

or

$$(1 - \mathcal{P}) \begin{pmatrix} \mathrm{e}_z^{\mathrm{sp}} \\ \mathrm{h}_t^{\mathrm{sp}} \end{pmatrix} = 0 = (1 - \mathcal{F}) \begin{pmatrix} \mathrm{e}_z^{\mathrm{sp}} \\ \mathrm{h}_t^{\mathrm{sp}} \end{pmatrix}. \tag{12}$$

The left and right equalities in (11) are satisfied when $\mathrm{h}_t^{\mathrm{sp}} = \mathcal{Y}_0 \mathrm{e}_z^{\mathrm{sp}}$ and $\mathrm{h}_t^{\mathrm{sp}} = -\mathcal{Y}_1 \mathrm{e}_z^{\mathrm{sp}}$, respectively. Hence, non-trivial solutions will exist if the null-space $\mathcal{N}(\mathcal{Y}_0 + \mathcal{Y}_1)$ is non-empty. Equivalently, from (12), it follows that the corresponding spurious solutions must simultaneously satisfy $\mathrm{h}_t^{\mathrm{sp}} = \big(\mathcal{Y}_0 + \mathcal{G}_0^{-1}\big)\, \mathrm{e}_z^{\mathrm{sp}}$ and $\mathrm{h}_t^{\mathrm{sp}} = \mathcal{Y}_1 \mathrm{e}_z^{\mathrm{sp}}$, which in turn is feasible if the null-space $\mathcal{N}\big(\widetilde{\mathcal{Y}}_0 + \mathcal{Y}_1\big)$ is non-empty. Simulations suggest that only spurious solutions that satisfy (12) can be found. To prove this, we show that null-space $\mathcal{N}\big(\mathcal{Y}_0 + \mathcal{Y}_1\big)$ is always empty by applying the same steps as above for the well-known, resonance-free PMCHWT formulation

$$\left(\mathcal{P} - \big(1 - \widetilde{\mathcal{P}}_1\big)\right) \begin{pmatrix} \mathrm{e}_z^+ \\ \mathrm{h}_t^+ \end{pmatrix} = \begin{pmatrix} \mathrm{e}_z^{\mathrm{in}} \\ \mathrm{h}_t^{\mathrm{in}} \end{pmatrix}, \tag{13}$$

with the BIE formulation in $S$ represented by $\mathcal{P}_1$ for fields on $C^-$, or equivalently, by $1 - \widetilde{\mathcal{P}}_1$ for fields on $C^+$. Analysis of the eigensolutions of $\mathcal{P}$ and $1 - \widetilde{\mathcal{P}}_1$ shows that the elements of the null-space $\mathcal{N}\big(\mathcal{Y}_0 + \mathcal{Y}_1\big)$ are spurious modes of (13). Since this PMCHWT formulation is known to be resonance-free, we conclude that this null-space will be empty, at least for $S$ formed by isotropic and piecewise homogeneous materials.

We proved that the elements of the null-space $\mathcal{N}\big(\widetilde{\mathcal{Y}}_0 + \mathcal{Y}_1\big)$ will be spurious modes of (10), and for some specific cross-sectional shapes $S$ with closed-form analytic expressions for $\widetilde{\mathcal{Y}}_0$ and $\mathcal{Y}_1$, the breakdown frequencies of (10) can be predicted. This is demonstrated in Section IV for a circular cross-section $S$, and the simulations of the cylindrical TM scattering example confirm that all resonances occur at singular frequencies of $\widetilde{\mathcal{Y}}_0 + \mathcal{Y}_1$, with the spurious modes satisfying (12).

Finally, for reference, we provide a resonance-free formulation that uses the Robin-to-Robin boundary conditions $\mathrm{e}_z^- + \mathrm{h}_t^- = \mathrm{e}_z^+ - \mathrm{h}_t^+$ and $\mathrm{e}_z^- - \mathrm{h}_t^- = \mathrm{e}_z^+ + \mathrm{h}_t^+$ between $C^-$ and $C^+$. As described in [4], the hybrid FE-BIE formulation using the MFF with Robin boundary conditions is given by

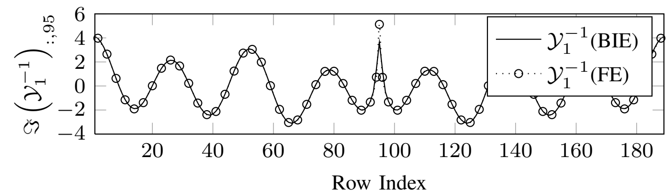


Fig. 1. Imaginary part of the 95th column of the discretized $\mathcal{Y}_1^{-1}$ PS operator for $S$, $f_0 = 300\,\mathrm{MHz}$, obtained from the BIE method (solid) and the FE method after compressing the system matrix (dotted).

$$\begin{pmatrix} \frac{-1}{2} & \frac{-1}{2} & \frac{1}{2} & \frac{-1}{2} \\ \frac{-1}{2} & \mathcal{Y}_1^{-1} + \frac{1}{2} & \frac{-1}{2} & \frac{1}{2} \\ \frac{1}{2} & \frac{-1}{2} & \frac{-1}{2} - \mathcal{J}_0 & \mathcal{K}_0' \\ \frac{-1}{2} & \frac{1}{2} & \mathcal{K}_0 & \frac{1}{2} - \mathcal{G}_0 \end{pmatrix} \begin{pmatrix} \mathrm{e}_z^- \\ \mathrm{h}_t^- \\ \mathrm{e}_z^+ \\ \mathrm{h}_t^+ \end{pmatrix} = \begin{pmatrix} 0 \\ 0 \\ \mathrm{h}_t^{\mathrm{in}} \\ -\mathrm{e}_z^{\mathrm{in}} \end{pmatrix}. \tag{14}$$

Besides (14), other, unsymmetric resonance-free formulations exist, like the formulation used in [5].

## IV. Numerical Results

To illustrate the above concepts, consider a dielectric cylinder, embedded in free space and with a circular cross-section $S$ of radius $R = 1\,\mathrm{m}$. The cylinder is formed by the homogeneous and isotropic material with relative material parameters $(\epsilon_r, \mu_r) = (2, 1)$, allowing us to compare with the BIE-only PMCHWT formulation in terms of robustness and accuracy. The boundary is approximated by 189 segments of equal length $l$, while the interior of $S$ is triangulated into a high-quality mesh featuring 6705 faces of typical element size $l$. To discretize the BIE operators, we employ a consistent Petrov-Galerkin method, with linear rooftop functions $w_t$ as basis for $\mathrm{e}_z^+$ and piecewise constant basis functions $w_p$ for $\mathrm{h}_t^+$, and test (1) and (2) with $w_p$ and $w_t$, respectively. In the FE method, we use scalar node basis and testing functions $w_n$ for the EFF and edge basis and testing functions $\mathbf{w}_e$ for the MFF.

To illustrate the numerical equivalence between the compressed MFF FE system matrix and the discretized PS operator $\mathcal{Y}_1^{-1}$, we use the BIE formalism in $S$ to obtain

$$\mathcal{Y}_1^{-1} = \mathcal{G}_1 - \left(\mathcal{K}_1 - \tfrac{1}{2}\right) \mathcal{J}_1^{-1} \left(\mathcal{K}_1 + \tfrac{1}{2}\right). \tag{15}$$

Fig. 1 compares the 95th column of the compressed FE matrix and the discrete PS operator from (15) for $f_0 = 300\,\mathrm{MHz}$, and the link between the FE system matrix and the PS operator is confirmed. The small error at row index 95 is due to numerical issues with the hypersingular self-patch contribution.

To verify the theory of Section III, we illuminate the cylinder with a time-harmonic plane wave with wave number $k_0 = 2\pi f_0 \sqrt{\epsilon_0 \mu_0}$, traveling along the positive $x$-axis. An analytical expression for $\mathcal{Y}_1$ or $\widetilde{\mathcal{Y}}_0$ is easily found from the eigensolutions of the Laplace operator $\nabla_t^2$ in cylindrical coordinates $(\rho, \phi)$. Writing $\mathrm{e}_z^+$ and $\mathrm{h}_t^+$ as a complex Fourier series with respective coefficients $c_n J_n(k_1 R)$ and $c_n J_n'(k_1 R)$, the equivalent $\mathcal{Y}_1$ operator for the $n$-th term is

$$\mathcal{Y}_{1,n} = -j \sqrt{\frac{\epsilon_r}{\mu_r}} \frac{J_n'(k_1 R)}{J_n(k_1 R)}, \tag{16}$$

TABLE I
THEORETICAL RESONANCE FREQUENCIES AND CORRESPONDING MODE NUMBERS $n;m$ OF THE DIFFERENT FE-BIE FORMULATIONS.

| $\widetilde{\mathcal{Y}}_0$ | | $\widetilde{\mathcal{Y}}_0^{-1}$ | | $\widetilde{\mathcal{Y}}_0 + \mathcal{Y}_1$ | |
|---|---|---|---|---|---|
| $f_0$ [MHz] | $n;m$ | $f_0$ [MHz] | $n;m$ | $f_0$ [MHz] | $n;m$ |
| 87.8492 | 1;1 | 114.7425 | 0;1 | 70.9312 | 1;1 |
| 145.7282 | 2;1 | 182.8239 | 1;1 | 96.2430 | 0;1 |
| 182.8239 | 0;1 | 245.0383 | 2;1 | 116.7053 | 2;1 |
| 200.4532 | 3;1 | 263.3820 | 0;2 | 150.1211 | 0;2 |
| 253.7188 | 4;1 | 304.4195 | 3;1 | 152.8110 | 1;2 |
| 254.3815 | 1;2 | 334.7379 | 1;2 | 159.4760 | 3;1 |

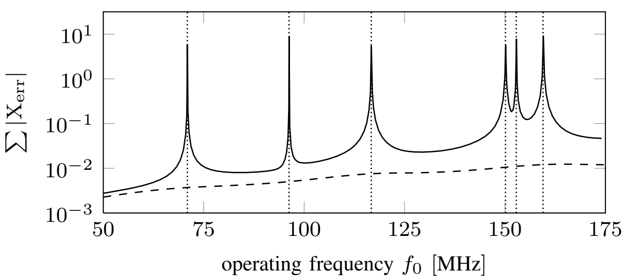


Fig. 2. L1-norm of the combined error $X_{err}$ in $(e_z^+, h_t^+)$ w.r.t. the reference PMCHWT solution for the FE-BIE formulations (10) (solid) and (14) (dashed), and the theoretical resonance frequencies (dotted).

with $k_1 = k_0\sqrt{\epsilon_r \mu_r}$ and $J_n'$ the derivative with respect to the argument of the $n$-th order Bessel function of the first kind. From (16), the Neumann and Dirichlet eigenfrequencies for the exterior resonances are easily obtained as the roots of $J_n'(k_0R)$ and $J_n(k_0R)$, respectively. In a similar manner, the breakdown frequencies of (10) are found as the roots of

$$J_n'(k_0R)\, J_n(k_1R) + \sqrt{\tfrac{\epsilon_r}{\mu_r}} J_n(k_0R)\, J_n'(k_1R)\,,$$

and in Table I, the first 6 resonance frequencies of $\widetilde{\mathcal{Y}}_0$, $\widetilde{\mathcal{Y}}_0^{-1}$ and $\widetilde{\mathcal{Y}}_0 + \mathcal{Y}_1$ are listed together with the corresponding mode number $n;m$ ($m$-th zero of order $n$). In Fig. 2, we observe that the theoretical breakdown frequencies of $\widetilde{\mathcal{Y}}_0 + \mathcal{Y}_1$ (dotted) indeed correspond to the frequencies where the solution error for (10) is maximized (solid), while the formulation with Robin boundary conditions (dashed) remains unaffected.

Besides the solution error due to the spurious modes, a frequency dependent dispersion error is introduced by the finite mesh in $S$. Compared to the node basis functions, the edge basis functions provide a better approximation of the inner field interactions, hence the MFF will generally provide more accurate results than the EFF. In Fig. 3, we compare the combined error in $e_z^+$ and $h_t^+$ with respect to the reference PMCHWT solution for different FE-BIE formulations. Besides the spurious solutions in some formulations, it is observed that all formulations introduce an increasing dispersion error as a function of frequency, and that the edge basis functions in the MFF indeed provide the most accurate results, which follows from comparing the formulation with the EFF and Robin boundary conditions (dash-dotted) with the formulation with the MFF and Robin boundary conditions (dashed).

Without Robin boundary conditions, spurious solutions introduce large errors in the neighborhood of specific breakdown frequencies. For the EFF- and MFF-only formulations, these neighborhoods are very small, and these formulations are therefore rather robust. However, when the EFF and the MFF are combined as in (10), the influence of the spurious solutions are observed in a much larger frequency interval, as shown in Fig. 3 for formulation (10) (solid). For the same mesh, the edge and node basis functions have a different interaction pattern, hence the field propagation in $S$ is approximated differently, and the small difference between the numerical wave numbers broadens the frequency range over which spurious modes can exist. This effect can be avoided by discretizing only the operator $\mathcal{Y}_1^{-1}$ in the MFF, after which we can invert the resulting system matrix to form the discrete equivalent of $\mathcal{Y}_1$, but now with the same approximated wave number. As observed in Fig. 3, the resulting formulation (denoted MFF$^{-1}$+MFF) (dotted) is indeed more robust and has an equivalent dispersion error as the MFF-only formulation with Robin boundary conditions. However, besides the fact that the breakdown frequencies are still present in the MFF$^{-1}$+MFF formulation, the matrix inversion can lead to numerical problems when the compressed MFF system matrix is singular.

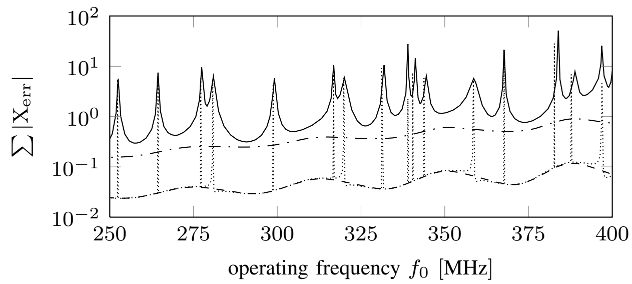


Fig. 3. L1-norm of the combined error $X_{err}$ in $(e_z^+, h_t^+)$ w.r.t. the reference PMCHWT solution for the FE-BIE formulations with EFF+MFF (solid), MFF$^{-1}$+MFF (dotted), EFF Robin (dash-dotted) and MFF Robin (dashed).

## V. Conclusion

By identifying the FE formulation with a PS operator, an operator notation for hybrid FE-BIE formulations can be constructed that provides remarkable theoretical insight regarding accuracy and the existence of breakdown frequencies. We showed the equivalence between the compressed FE matrix and the discretized PS operator, and verified the theory on a TM scattering problem where we successfully predicted the breakdown frequencies of a specific FE-BIE formulation.

## References

[1] L. Knockaert, D. De Zutter, G. Lippens, and H. Rogier, "On the schur complement form of the dirichlet-to-neumann operator," *Wave Motion*, vol. 45, no. 3, pp. 309–324, 2008.
[2] S.-C. Lee, M. N. Vouvakis, K. Zhao, and J.-F. Lee, "Analysing microwave devices using a symmetric coupling of finite and boundary elements," *International Journal for Numerical Methods in Engineering*, vol. 64, no. 4, pp. 528–546, 2005.
[3] A. Mitchell, D. Kokotoff, and M. Austin, "Closed-form expressions for the numerical dispersion and reflection in FEM simulations involving biaxial materials," *IEEE Trans. Antennas Propag.*, vol. 49, no. 2, pp. 158–164, 2001.
[4] K. Zhao, M. N. Vouvakis, and J.-F. Lee, "Solving electromagnetic problems using a novel symmetric FEM-BEM approach," *IEEE Trans. Magn.*, vol. 42, no. 4, pp. 583–586, 2006.
[5] A. Tzoulis and T. F. Eibert, "A hybrid FEBI-MLFMM-UTD method for numerical solutions of electromagnetic problems including arbitrarily shaped and electrically large objects," *IEEE Trans. Antennas Propag.*, vol. 53, no. 10, pp. 3358–3366, 2005.